



Deposited via The University of Leeds.

White Rose Research Online URL for this paper:

<https://eprints.whiterose.ac.uk/id/eprint/94095/>

Version: Accepted Version

---

**Article:**

Pal, A, Potjer, TP, Thomsen, SK et al. (2016) Loss-of-Function Mutations in the Cell-Cycle Control Gene CDKN2A Impact on Glucose Homeostasis in Humans. *Diabetes*, 65 (2). pp. 527-533. ISSN: 0012-1797

<https://doi.org/10.2337/db15-0602>

---

**Reuse**

Items deposited in White Rose Research Online are protected by copyright, with all rights reserved unless indicated otherwise. They may be downloaded and/or printed for private study, or other acts as permitted by national copyright laws. The publisher or other rights holders may allow further reproduction and re-use of the full text version. This is indicated by the licence information on the White Rose Research Online record for the item.

**Takedown**

If you consider content in White Rose Research Online to be in breach of UK law, please notify us by emailing [eprints@whiterose.ac.uk](mailto:eprints@whiterose.ac.uk) including the URL of the record and the reason for the withdrawal request.

## Loss-of-Function Mutations in the Cell-Cycle Control Gene *CDKN2A* Impact on Glucose Homeostasis in Humans

Short running title: The role of *CDKN2A* in glucose homeostasis

Aparna Pal<sup>1\*</sup>, Thomas P. Potjer<sup>2\*</sup>, Soren K. Thomsen<sup>1\*</sup>, Hui Jin Ng<sup>1</sup>, Amy Barrett<sup>1</sup>, Raphael Scharfmann<sup>3</sup>, Tim J. James<sup>4</sup>, D. T. Bishop<sup>5</sup>, Fredrik Karpe<sup>1,6</sup>, Ian F. Godsland<sup>7</sup>, Hans F.A. Vasen<sup>8</sup>, Julia Newton-Bishop<sup>5</sup>, Hanno Pijl<sup>9</sup>, Mark I. McCarthy<sup>1,6,10</sup>, Anna L. Gloyn<sup>1,6</sup>

\*A.P, T.P.P and S.K.T. are joint first authors.

- 1) Oxford Centre for Diabetes Endocrinology & Metabolism, University of Oxford, UK
- 2) Department of Clinical Genetics, Leiden University Medical Center, Leiden, Netherlands
- 3) INSERM U1016, Institut Cochin, Université Paris Descartes, Paris, France
- 4) Department of Clinical Biochemistry, John Radcliffe Hospital, Oxford, UK
- 5) Leeds Institute of Cancer & Pathology, University of Leeds, Leeds, UK
- 6) Oxford NIHR Biomedical Research Centre, Churchill Hospital, Oxford, UK
- 7) Diabetes, Endocrinology and Metabolism, Department of Medicine, Imperial College London, London, UK
- 8) Department of Gastroenterology & Hepatology, Leiden University Medical Center, Leiden, Netherlands
- 9) Leiden University Medical Centre, Department of Internal Medicine, Leiden, Netherlands
- 10) Wellcome Trust Centre for Human Genetics, University of Oxford, UK

### Address for Correspondence

Professor Anna L Gloyn  
Oxford Centre for Diabetes Endocrinology & Metabolism  
Churchill Hospital, Oxford, OX3 7LE, UK  
Tel:- +44 1865 857298  
Fax:- +44 1865 857299  
Email:- [Anna.Gloyn@drl.ox.ac.uk](mailto:Anna.Gloyn@drl.ox.ac.uk)

Number of Tables: 2

Number of Figures: 2

**1 Abstract**

2           At the *CDKN2A/B* locus, three independent signals for type 2 diabetes risk are located  
3 in a non-coding region near *CDKN2A*. The disease-associated alleles have been implicated in  
4 reduced  $\beta$ -cell function, but the underlying mechanism remains elusive. In mice,  $\beta$ -cell  
5 specific loss of *Cdkn2a* causes hyperplasia whilst overexpression leads to diabetes,  
6 highlighting *CDKN2A* as a candidate effector transcript. Rare *CDKN2A* loss-of-function  
7 mutations are a cause of familial melanoma and offer the opportunity to determine the impact  
8 of *CDKN2A* haploinsufficiency on glucose homeostasis in humans. To test the hypothesis  
9 that such individuals have improved  $\beta$ -cell function, we performed oral and intravenous  
10 glucose tolerance tests on mutation carriers and matched controls. Compared with controls,  
11 carriers displayed increased insulin secretion, impaired insulin sensitivity and reduced hepatic  
12 insulin clearance. These results are consistent with a model whereby *CDKN2A*-loss affects a  
13 range of different tissues, including pancreatic  $\beta$ -cells and liver. To test for direct effects of  
14 *CDKN2A*-loss on  $\beta$ -cell function, we performed knockdown in a human  $\beta$ -cell line, EndoC-  
15 bH1. This revealed increased insulin secretion independent of proliferation. Overall, we  
16 demonstrate that *CDKN2A* is an important regulator of glucose homeostasis in humans, thus  
17 supporting its candidacy as an effector transcript for type 2 diabetes-associated alleles in the  
18 region.

## 19 Introduction

20 Non-coding genetic signals at the *CDKN2A/B* locus have been associated with  
21 increased risk of developing type 2 diabetes (1, 2). One signal is contained within a long non-  
22 coding RNA (*ANRIL*), while two distinct signals map to a region located further upstream of  
23 *CDKN2A* and *CDKN2B*. Physiological characterisations of normoglycemic carriers have  
24 demonstrated that the risk alleles are associated with reduced  $\beta$ -cell function, yet the  
25 underlying ‘effector’ transcript driving these effects has not been established (3, 4).

26 *CDKN2A* encodes the alternatively spliced proteins p16<sup>INK4a</sup> and p14<sup>ARF</sup>, which are  
27 known tumour suppressors acting via distinct signalling pathways (5, 6). p16<sup>INK4a</sup> is a cyclin-  
28 dependent kinase inhibitor (CDKI) involved in the regulation of cell cycle progression  
29 through inhibition of CDK4 and CDK6 (7). p14<sup>ARF</sup>, in contrast, prevents the degradation of  
30 the cell-cycle regulator p53 by forming a stable complex with Mdm2 in the nucleus (8).

31 Rodent studies have linked *Cdkn2a* to glucose homeostasis, pointing to the gene as a  
32 plausible candidate effector transcript at the *CDKN2A/B* locus. In a  $\beta$ -cell specific knockout  
33 mouse, *Cdkn2a* deficiency was found to increase  $\beta$ -cell proliferation and conferred resistance  
34 to chemically-induced diabetes (9). Overexpression, in contrast, reduced  $\beta$ -cell proliferation  
35 in both young and old mice. This is consistent with the effect of *Cdk4*-loss, which has been  
36 shown to result in a reduced number of pancreatic  $\beta$ -cells and insulin-deficient diabetes (10).  
37 More recent mouse studies have also established a role for *Cdkn2a* and *Cdk4* in hepatic  
38 glucose production (HGP), demonstrating cell-cycle independent effects on gluconeogenesis  
39 under fasted and fed conditions (11, 12).

40 While rodent studies have provided critical clues into the contribution of *Cdkn2a* to  
41 diabetes pathogenesis, less is known about the role of *CDKN2A* in glucose homeostasis in  
42 humans. The machinery regulating the G1/S transition in adult human  $\beta$  cells differs from

43 that of mouse  $\beta$  cells, which do not express CDK6 (13-15). Individuals heterozygous for  
44 germline loss-of-function mutations in the *CDKN2A* gene have a high risk of developing  
45 (multiple) cutaneous melanoma, a condition known as familial atypical multiple mole  
46 melanoma syndrome (FAMMM) (16, 17). These subjects provide a unique opportunity to  
47 study the effect of *CDKN2A* haploinsufficiency on glucose homeostasis in humans. The  
48 present study tested the hypothesis that mutation carriers show improved  $\beta$ -cell function  
49 compared with non-carriers.

## 50 **Research design and methods**

### 51 *Study participants*

52           Thirty-one cases diagnosed with FAMMM due to *CDKN2A* mutations were recruited  
53 from centres in the UK and the Netherlands. Twenty-eight had been cancer free for at least  
54 two years, and the remaining three cases had presented with melanoma between four to  
55 twelve months prior to inclusion in the study (**supplementary table 1**). For a control group  
56 of thirty-one participants, unaffected first-degree relatives or spouses of carriers were chosen  
57 when available and additional controls were recruited from the Oxford Biobank  
58 ([www.oxfordbiobank.org.uk](http://www.oxfordbiobank.org.uk)). Two controls were subsequently excluded based on 2-h OGTT  
59 glucose levels diagnosing diabetes (serum glucose >11 mmol/L). All remaining participants  
60 were aged 18-80 years, not suffering from diabetes, and not taking any medication that could  
61 interfere with glucose tolerance.

### 62 *Baseline clinical characteristics and oral glucose tolerance test (OGTT)*

63           All participants underwent a 75 g OGTT following a 12 hour fast. Blood samples  
64 were collected at 0, 15, 30, 60, 90 and 120 min after the oral glucose load to assay plasma  
65 glucose, serum insulin and (for a subset of twelve mutation carriers and twelve controls) also  
66 C-peptide. Insulin and C-peptide were measured using chemiluminescence immunoassays.  
67 Measures of insulin sensitivity,  $\beta$ -cell function and hepatic clearance derived from the OGTT  
68 were calculated according to the formulae in **supplementary table 2**.

### 69 *Intravenous glucose tolerance test (IVGTT)*

70           IVGTTs were performed on a subset of the UK subjects (eight) who had attended for  
71 OGTT and consented to undergo an IVGTT. Control subjects, matched for age, gender, BMI  
72 and activity were recruited from the Oxford Biobank. Following a 12 hour fast, a dose of 50

73 % dextrose (calculated based on weight 0.5mg/kg) was given over 3 minutes. Blood samples  
74 were then taken at 0, 2, 4, 6, 8, 10, 15, 20, 30, 45, 60, 75, 90, 120, 150 and 180 minutes.  
75 These samples were batch-analysed for insulin, glucose and C-peptide. Data were then  
76 analysed using a minimal model approach, according to an algorithm designed to maximise  
77 precision and identification success rate (18).

#### 78 *Cellular assays using the EndoC-bH1 cell line*

79 The EndoC-bH1 cell line was cultured and passaged as previously described (19).  
80 Reverse transfections were performed by adding pre-formed siRNA complexes prepared  
81 from ON-TARGETplus siRNA SMARTpools (Dharmacon) at a final concentration of 10 nM  
82 siRNA. For gene expression analysis, RNA was extracted and quantitative PCR (qPCR)  
83 performed using the TaqMan gene expression kit and assays (Applied Biosystems) on oligo-  
84 dT primed cDNA. 72 h after transfection, cells were starved overnight in 2.8 mM glucose  
85 followed by 1 h in 0 mM glucose medium. Static insulin secretion assays were then initiated  
86 by adding glucose-free growth medium supplemented with the indicated amounts of glucose  
87 and IBMX. After 1 h, aliquots of supernatants were removed for later analysis, and ice-cold  
88 acid ethanol added to extract insulin content from cells. Sample analysis was performed using  
89 the AlphaLISA Human Insulin Immunoassay (Perkin Elmer).

90 For protein kinase A (PKA) activity assays, cells were harvested following knockdown, as  
91 described above, and washed in phosphate-buffered saline. Matching input for number of  
92 cells, the samples were then processed according to manufacturer's instructions for the  
93 PepTag non-radioactive PKA assay (Promega), and visualized using the ChemiDoc MP  
94 system.

#### 95 *Statistical analysis*

96 Statistical analysis was performed using R 3.0.2. P-values were determined by Welch's t-test,  
97 except for gender differences where the Chi-squared test was used and for analysis of the  
98 IVGTT data where the Mann-Whitney U test was used.

99

## 100 Results

101 We recruited thirty-one participants carrying inherited *CDKN2A* loss-of-function  
102 mutations (**supplementary table 1**) and thirty-one controls, matched as a group for age ( $p =$   
103 0.99), gender ( $p = 0.43$ ) and BMI ( $p = 0.97$ ) (**table 1**). To test our hypothesis that *CDKN2A*-  
104 loss leads to improved  $\beta$ -cell function, we first performed a 120-min oral glucose tolerance  
105 test (OGTT) in all subjects (**figure 1a-b**). While no difference in glucose levels was detected,  
106 insulin levels were significantly increased in carriers throughout the test ( $p = 0.01$  for insulin  
107 area under curve [AUC]; **table 2**).

108 Using these data, we derived standard indices of  $\beta$ -cell function and insulin sensitivity  
109 (**table 2**). This revealed increased  $\beta$ -cell function in carriers compared with non-carriers, both  
110 using a dynamic measure of acute insulin response ( $p = 0.03$  for BIGTT-AIR), and in the  
111 fasted state ( $p = 0.05$  for HOMA-B, homeostatic model assessment of  $\beta$ -cell function).  
112 Corresponding measures of insulin sensitivity, BIGTT-S and HOMA-S (homeostatic model  
113 assessment of insulin sensitivity), were also both found to be lower in carriers ( $p = 0.04$  and  $p$   
114  $= 0.05$ , respectively). Other standard measures, the Belfiore and Matsuda ISIs, confirmed the  
115 observed reduction in insulin sensitivity of carriers ( $p = 0.02$  and  $p = 0.02$ , respectively). As a  
116 result, the disposition index, which is an aggregate measure of  $\beta$ -cell function relative to  
117 glucose sensitivity, remained unaffected compared with controls ( $p = 0.98$ ). These results  
118 were not significantly altered by exclusion of three carriers that had presented with melanoma  
119 within two years prior to inclusion in the study (**supplementary table 3**).

120 To explore whether the observed phenotype was driven by underlying effects on  
121  $p16^{\text{INK4a}}$ ,  $p14^{\text{ARF}}$  or both, we re-analysed the data grouping carriers by mutation status  
122 (**supplementary figure 1**). Of the mutations identified, 26 affected both  $p16^{\text{INK4a}}$  and  $p14^{\text{ARF}}$ ,  
123 while five were located in regions affecting  $p16^{\text{INK4a}}$  exclusively. No differences were  
124 observed between these two groups in insulin or glucose levels ( $p = 1.00$  for  $\text{AUC}_{\text{ins}}$  and  $p =$

125 0.49 for  $AUC_{\text{glucose}}$ , respectively), suggesting that the observed metabolic phenotype of  
126 mutation carriers may be driven either solely by effects on p16<sup>INK4a</sup>, or by effects of similar  
127 magnitude on both proteins.

128 For a subset of participants (twelve carriers and twelve controls) C-peptide  
129 measurements were obtained during the OGTT. Despite a tendency towards increased C-  
130 peptide levels in the fasted state ( $p = 0.48$ ), the total response was not different for this subset  
131 of individuals ( $p = 1.00$  for AUC). Indices of hepatic insulin clearance, derived from the ratio  
132 between C-peptide and insulin levels, however, showed significantly decreased hepatic  
133 clearance in mutation carriers ( $p = 0.03$ ; **table 2**) (20).

134 To confirm these findings, we performed IVGTTs on eight cases and eight controls  
135 available for follow-up studies (**supplementary figure 2**). None of the measures derived  
136 from this test reached statistical significance, but directions of effect were confirmed for both  
137 insulin secretion ( $p = 0.14$  for  $AUC_{\text{insulin}}$  10-180 min) and hepatic insulin clearance ( $p = 0.21$ )  
138 (**supplementary table 4**). The insulin response was found to be 66 % and 110 % higher for  
139 carriers during the first and second phase of secretion, respectively. In contrast, the C-peptide  
140 response (which is unaffected by hepatic clearance) was around 30 % higher during both  
141 phases of secretion, indicating a direct contribution of improved  $\beta$ -cell function to the  
142 elevated circulating insulin levels of carriers.

143 Finally, we sought to establish the extent to which cell-cycle independent effects of  
144 *CDKN2A* on the regulation of insulin secretion could contribute to the phenotype of mutation  
145 carriers. Recent work in rodent hepatocyte models has suggested a role of *CDKN2A* in the  
146 regulation of protein kinase A (PKA) signalling (12). Given the well-characterised effects of  
147 PKA on potentiation of insulin secretion, we speculated that such signalling events could  
148 have a direct effect on  $\beta$ -cell function. To test this hypothesis, we performed knockdown and

149 secretion studies in the human pancreatic  $\beta$ -cell line, EndoC-bH1. This cell line was  
150 transformed by Ravassard et al using the proto-oncogene SV40LT, which acts on the  
151 Retinoblastoma protein (Rb), thereby masking effects of p16<sup>INK4a</sup> on cell-cycle control (19).

152 We first confirmed expression of p16<sup>INK4a</sup> by immunofluorescence and found that,  
153 consistent with previous reports, the protein localized to both the nucleus and cytoplasm  
154 (**supplementary figure 3**) (21, 22). siRNA-mediated silencing of *CDKN2A* was then  
155 performed and efficient knockdown observed both at the mRNA and protein level (**figure 2a-**  
156 **b; supplementary figure 4**). 96 hours after gene silencing, cells treated with *CDKN2A* or  
157 non-targeting siRNAs were incubated under different conditions to assess the glucose-  
158 responsiveness of the cells. In addition to basal and high-glucose conditions, the effect of the  
159 phosphodiesterase inhibitor (IBMX) on insulin secretion was tested. For all three conditions,  
160 *CDKN2A* knockdown was found to increase insulin secretion as a fraction of total content  
161 (basal,  $p = 0.02$ ; high,  $p = 0.01$ ; high glucose with IBMX,  $p = 0.04$ ; **figure 2c-d**) and, as  
162 expected, no effect on proliferation was detected. We also observed a small, but significant  
163 reduction in the total insulin content per cell ( $p < 0.01$ ; **supplementary figure 5**). Finally, we  
164 performed PKA activity assays to directly assess the effect of *CDKN2A* silencing on the  
165 potentiating pathway of insulin secretion. Consistent with an increase in insulin secretion, this  
166 revealed a corresponding 23 % increase in the activity of PKA following *CDKN2A*  
167 knockdown ( $p = 0.02$ ; **supplementary figure 6**).

## 168 Discussion

169 Individuals carrying heterozygous loss-of-function mutations in the *CDKN2A* gene  
170 provide a unique opportunity to study the role of p16<sup>INK4a</sup> and p14<sup>ARF</sup> in glucose homeostasis  
171 in humans. Through oral and intravenous glucose tolerance tests, we found that carriers  
172 displayed significantly increased insulin levels compared with matched controls. In a subset

173 of individuals, measurements of C-peptide levels established a contribution of both decreased  
174 hepatic insulin clearance and increased  $\beta$ -cell function to the elevated circulating insulin.  
175 Further, grouping carriers by mutation status showed the effects to be driven either by  
176 p16<sup>INK4a</sup> exclusively or through similar effects on both p16<sup>INK4a</sup> and p14<sup>ARF</sup>.

177 Overall, these results are consistent with a combination of two, non-mutually  
178 exclusive mechanisms underlying the phenotype of carriers: (a) primary  $\beta$ -cell hyperfunction  
179 driving progressive insulin resistance; and/or (b) primary insulin resistance triggering a  
180 compensatory increase in insulin levels (**supplementary figure 7**). While both explanations  
181 are consistent with our data, existing evidence strongly support a role for *CDKN2A* in  $\beta$ -cell  
182 function (9). Chronic hyperinsulinemia is known to result in a gradual down-regulation of  
183 both insulin receptors and post-receptor signalling efficiency, thereby causing general insulin  
184 resistance and reduced insulin clearance (23). Our data are therefore in agreement with the  
185 expected physiological adaptation to chronic hyperinsulinemia. However, due to limitations on  
186 the design of our clinical study, we cannot conclusively address the cause and effect between  
187 hyperinsulinemia and insulin resistance in mutation carriers. The IVGTT is well validated  
188 against clamp-based techniques, but power calculations based on our results suggest that an  
189 impractically high number of 50-60 individuals would be required to establish significant  
190 differences. Given the rarity of the disease, this exceeds the number of carriers available in  
191 the UK and Dutch cohorts recruited for our study.

192 To test for a cell-cycle independent role of *CDKN2A* in the regulation of insulin  
193 secretion, we performed knockdown studies in the human  $\beta$ -cell line, EndoC-bH1. This  
194 identified cell-cycle independent increases in insulin secretion under three conditions. These  
195 changes were found to be accompanied by increased PKA activity, in agreement with  
196 previous studies establishing such an effect of *CDKN2A* knockdown in liver (11, 12). This  
197 suggests a possible contribution of the PKA-dependent potentiating pathway to the secretory

198 effects observed in the EndoC-bH1 cell line. Taken in combination with existing data, our  
199 clinical and cellular studies indicate that the phenotype of carriers may arise out of a complex  
200 interplay between both cell-cycle independent and dependent roles of *CDKN2A* in a range of  
201 tissues (**supplementary figure 7**) (9, 12).

202 Upstream of the *CDKN2A* and *CDKN2B* genes, several independent association  
203 signals for type 2 diabetes risk have been identified. The underlying effector transcript and  
204 disease mechanism has remained elusive, and prior studies have not reported any cis-  
205 expression quantitative trait loci (cis-eQTL) effects for these alleles (24). Our study has  
206 shown that both coding *CDKN2A* mutations and the non-coding type 2 diabetes variants are  
207 associated with effects on measures of  $\beta$ -cell function. This provides a link between  
208 *CDKN2A* and the common GWAS alleles, and thus points to the gene as a likely effector  
209 transcript at this locus.

210 Interestingly, type 2 diabetes-associated variants at the *CDKN2A/B* locus have  
211 consistently been linked to a more ‘classic’  $\beta$ -cell phenotype than that observed for carriers of  
212 coding mutations in our study, with no evidence for an impact on measures of insulin  
213 resistance (3, 4). We speculated that any cis-regulatory effect exerted on *CDKN2A* could  
214 achieve a more restricted  $\beta$ -cell phenotype through tissue-specific regulation of gene  
215 expression. To address this hypothesis, we interrogated existing genome annotations, and  
216 found that the non-coding disease-associated variants map to a cluster of islet enhancer  
217 activity and open chromatin. Specifically, the association signals overlap a strong enrichment  
218 for islet- and melanocyte-specific FOXA-2 binding (**supplementary figure 8**) (25). This  
219 highlights a possible mechanism for the more specific  $\beta$ -cell phenotype caused by common  
220 disease-associated variants compared with carriers of coding variants. Based on the direction  
221 of effect on measures of  $\beta$ -cell function, the non-coding risk alleles would be predicted to  
222 increase expression of *CDKN2A* (3, 4). No cis-eQTL effects have previously been reported in

223 islets for this region, but larger studies currently underway may be able to shed further light  
224 on this hypothesis (26).

225       Taken together, our data establish *CDKN2A* as an important regulator of glucose  
226 homeostasis in humans. We have shown that our data are consistent with loss-of-function  
227 mutations in *CDKN2A* affecting a range of tissues, including both pancreatic  $\beta$ -cells and  
228 liver. Our study thus supports the candidacy of *CDKN2A* as the effector transcript of the type  
229 2 diabetes-associated alleles in the region, and we have proposed a mechanism to account for  
230 the apparent tissue-specificity of the  $\beta$ -cell dysfunction caused by diabetes risk alleles.

**231 Acknowledgements**

232 The authors thank Linda Whitaker (University of Leeds) and Beryl Barrow (University of  
233 Oxford) for their valuable assistance with recruiting FAMMM patients in the UK, Marja  
234 Dijk, Bep Ladan and Petra Beckers (Leiden University Medical Centre) for assistance with  
235 performing the OGTTs in the Netherlands, and Jonathan Levy (University of Oxford) for  
236 advice on designing the study. We thank all volunteers in the UK and the Netherlands for  
237 their participation. The Oxford Biobank ([www.oxfordbiobank.org.uk](http://www.oxfordbiobank.org.uk)), NIHR Oxford  
238 Biomedical Research Centre, is part of the NIHR National Bioresource which supported the  
239 recalling process of the volunteers.

240 This study was funded by the Wellcome Trust (095101/Z/10/Z and 098381), the Medical  
241 Research Council (G0800467), the National Institute of Health Research Oxford Biomedical  
242 Research Centre, Cancer Research UK (C588/A19167) and the ZOLEON foundation (no  
243 12.09). ALG is a Wellcome Trust Senior Fellow in Basic Biomedical Science and MIM is a  
244 Wellcome Trust Senior Investigator. ALG is the guarantor of the data in this manuscript. The  
245 authors declare no conflicts of interest.

246

**247 Author Contributions**

248 AP, SKT, JNB, MIM, ALG conceived and designed the study. RS, TB provided protocols &  
249 clinical data. AP, TPP, SKT, AB, HJN performed the experiments. AP, ST, HJN, IFG  
250 analysed the data. AP, TPP, SKT, FK, IFG, HFAV, HP, MIM, ALG interpreted the data.  
251 SKT, ALG wrote the first draft of the manuscript. AP, TPP, MIM, HP edited the manuscript.  
252 AP, TPP, SKT, AB, HJN, RS, TJJ, IFG, TB, FK, HFAV, JNB, HP, MIM, ALG approved the  
253 final manuscript.

## References

- 1 Voight, B.F., *et al.* (2010) Twelve type 2 diabetes susceptibility loci identified through large-scale association analysis. *Nat Genet* 42, 579-589
- 2 Morris, A.P., *et al.* (2012) Large-scale association analysis provides insights into the genetic architecture and pathophysiology of type 2 diabetes. *Nat Genet* 44, 981-990
- 3 Grarup, N., *et al.* (2007) Studies of association of variants near the HHEX, CDKN2A/B, and IGF2BP2 genes with type 2 diabetes and impaired insulin release in 10,705 Danish subjects: validation and extension of genome-wide association studies. *Diabetes* 56, 3105-3111
- 4 Dimas, A.S., *et al.* (2014) Impact of type 2 diabetes susceptibility variants on quantitative glycemic traits reveals mechanistic heterogeneity. *Diabetes* 63, 2158-2171
- 5 Kamb, A., *et al.* (1994) A cell cycle regulator potentially involved in genesis of many tumor types. *Science* 264, 436-440
- 6 Kamijo, T., *et al.* (1997) Tumor suppression at the mouse INK4a locus mediated by the alternative reading frame product p19ARF. *Cell* 91, 649-659
- 7 Serrano, M., *et al.* (1993) A new regulatory motif in cell-cycle control causing specific inhibition of cyclin D/CDK4. *Nature* 366, 704-707
- 8 Weber, H.O., *et al.* (2002) Human p14(ARF)-mediated cell cycle arrest strictly depends on intact p53 signaling pathways. *Oncogene* 21, 3207-3212
- 9 Krishnamurthy, J., *et al.* (2006) p16INK4a induces an age-dependent decline in islet regenerative potential. *Nature* 443, 453-457
- 10 Rane, S.G., *et al.* (1999) Loss of Cdk4 expression causes insulin-deficient diabetes and Cdk4 activation results in beta-islet cell hyperplasia. *Nat Genet* 22, 44-52
- 11 Lee, Y., *et al.* (2014) Cyclin D1-Cdk4 controls glucose metabolism independently of cell cycle progression. *Nature* 510, 547-551
- 12 Bantubungi, K., *et al.* (2014) Cdkn2a/p16Ink4a regulates fasting-induced hepatic gluconeogenesis through the PKA-CREB-PGC1alpha pathway. *Diabetes* 63, 3199-3209
- 13 Martin, J., *et al.* (2003) Genetic rescue of Cdk4 null mice restores pancreatic beta-cell proliferation but not homeostatic cell number. *Oncogene* 22, 5261-5269
- 14 Fiaschi-Taesch, N., *et al.* (2009) Survey of the human pancreatic beta-cell G1/S proteome reveals a potential therapeutic role for cdk-6 and cyclin D1 in enhancing human beta-cell replication and function in vivo. *Diabetes* 58, 882-893
- 15 Fiaschi-Taesch, N.M., *et al.* (2010) Induction of human beta-cell proliferation and engraftment using a single G1/S regulatory molecule, cdk6. *Diabetes* 59, 1926-1936
- 16 Cannon-Albright, L.A., *et al.* (1992) Assignment of a locus for familial melanoma, MLM, to chromosome 9p13-p22. *Science* 258, 1148-1152
- 17 Goldstein, A.M. (2004) Familial melanoma, pancreatic cancer and germline CDKN2A mutations. *Hum Mutat* 23, 630
- 18 Godsland, I.F., *et al.* (2006) Evaluation of nonlinear regression approaches to estimation of insulin sensitivity by the minimal model with reference to Bayesian hierarchical analysis. *Am J Physiol Endocrinol Metab* 291, E167-174
- 19 Ravassard, P., *et al.* (2011) A genetically engineered human pancreatic beta cell line exhibiting glucose-inducible insulin secretion. *J Clin Invest* 121, 3589-3597
- 20 Horwitz, D.L., *et al.* (1975) Proinsulin, insulin, and C-peptide concentrations in human portal and peripheral blood. *J Clin Invest* 55, 1278-1283
- 21 McKenzie, H.A., *et al.* (2010) Predicting functional significance of cancer-associated p16(INK4a) mutations in CDKN2A. *Hum Mutat* 31, 692-701
- 22 Keller-Melchior, R., *et al.* (1998) Expression of the Tumor Suppressor Gene Product p16INK4 in Benign and Malignant Melanocytic Lesions. 110, 932-938
- 23 Shanik, M.H., *et al.* (2008) Insulin resistance and hyperinsulinemia: is hyperinsulinemia the cart or the horse? *Diabetes Care* 31 Suppl 2, S262-268
- 24 Hannou, S.A., *et al.* (2015) Functional genomics of the CDKN2A/B locus in cardiovascular and metabolic disease: what have we learned from GWASs? *Trends Endocrinol Metab* 26, 176-184
- 25 Pasquali, L., *et al.* (2014) Pancreatic islet enhancer clusters enriched in type 2 diabetes risk-associated variants. *Nat Genet* 46, 136-143
- 26 Fadista, J., *et al.* (2014) Global genomic and transcriptomic analysis of human pancreatic islets reveals novel genes influencing glucose metabolism. *Proc Natl Acad Sci U S A* 111, 13924-13929

	<b>Mutation carriers</b>	<b>Non-carriers</b>	<b>P-value</b>
n	31	31	<i>NA</i>
BMI / [cm/kg <sup>2</sup> ]	27.1 [19; 38]	27.1 [19; 36]	0.97
Age / [yrs]	51.8 [21; 71]	51.8 [25; 84]	0.99
Gender / [% male]	45	32	0.43

**Table 1** Baseline characteristics of study participants. Data are given as mean and range [min; max]. P-values are from Welch's t-test except for gender distribution where the Chi-squared test was performed.

	<b>Mutation carriers</b>	<b>Non-carriers</b>	<b>P-value</b>
Fasting glucose [mmol/L]	5.2 [4.3; 6.3]	5.1 [3.2; 6.4]	0.65
Fasting insulin [pmol/L]	87 [15; 337]	55 [22; 150]	0.01
Fasting C-peptide [nmol/L]	0.44 [0.24; 0.81]	0.39 [0.20; 0.60]	0.48
iHOMA-B	124 [38.1; 452.4]	96 [45; 236.7]	0.05
iHOMA-S	91 [18; 328.7]	120 [35; 235.6]	0.05
BIGTT-AIR [ $*10^3$ ]	6.4 [0.9; 28]	3.0 [1.2; 12]	0.03
BIGTT-S	5.8 [0.4; 12.8]	7.8 [1.1; 17.8]	0.04
Belfiore ISI	0.78 [0.17; 1.35]	0.97 [0.35; 1.77]	0.02
Matsuda ISI	4.3 [0.8; 11.1]	6.3 [1.5; 20.9]	0.02
AUC <sub>glucose</sub>	839 [563; 1449]	829 [502; 1086]	0.79
AUC <sub>insulin</sub> [ $*10^4$ ]	7.3 [2.4; 25]	4.7 [1.1; 15]	0.01
AUC <sub>C-Peptide</sub>	212 [106; 333]	212 [115; 260]	1.00
Insulinogenic index	203 [39; 561]	152 [53; 360]	0.08
C-peptidogenic index	0.45 [0.15; 1.12]	0.45 [0.17; 1.78]	1.00
Disposition index	2.3 [1.1; 3.8]	2.3 [1.0; 3.7]	0.98
Fasting insulin clearance	0.66 [0.12; 1.27]	0.88 [0.65; 1.29]	0.07
Insulin clearance	0.35 [0.16; 0.51]	0.56 [0.32; 1.05]	0.03

**Table 2** OGTT-derived measures of  $\beta$ -cell function, insulin sensitivity and hepatic clearance. Data are given as mean and range [min; max]. All indices based on C-peptide measurements are based on data from a subset of individuals only (n = 12 carriers and n = 12 controls; all UK). Details on definitions of physiological measures are listed in supplementary table 2.

**Figure legends**

**Figure 1** Serum glucose (*left panel*) and insulin (*right panel*) levels during a 120-min OGTT in thirty-one carriers (*black squares, solid line*) and thirty-one controls (*white circles, dashed line*). Data shown as mean +/- SEM.

**Figure 2** *CDKN2A* knockdown in the human  $\beta$ -cell line, EndoC-bH1. Silencing of *CDKN2A* (*white bars*) and non-targeting sequence (*black bars*) was performed using pools of siRNA (10 nM), and knockdown confirmed both at the mRNA level (*upper left panel*) and at the protein level (*upper right panel*) after 72 h. Static insulin secretion assays were performed under culturing conditions of basal glucose (2.8 mM glucose), high glucose (20 mM) and high glucose with IBMX (100  $\mu$ M) (*lower left panel*). All secretion results were normalized to total insulin content per well. Cellular proliferation (*lower right panel*) following treatment with si-*CDKN2A* (*white circles, dashed line*) and non-targeting siRNA (*black squares, solid line*) was measured using the CyQUANT Direct Cell Proliferation assay, and normalized to the respective counts on day 1. Bars represent means for n = 11 (si-*CDKN2A*) and 18 (non-targeting) generated in three independent experiments. Data points for cellular proliferation are means for n = 3, and error bars are SEM.

Figure 1

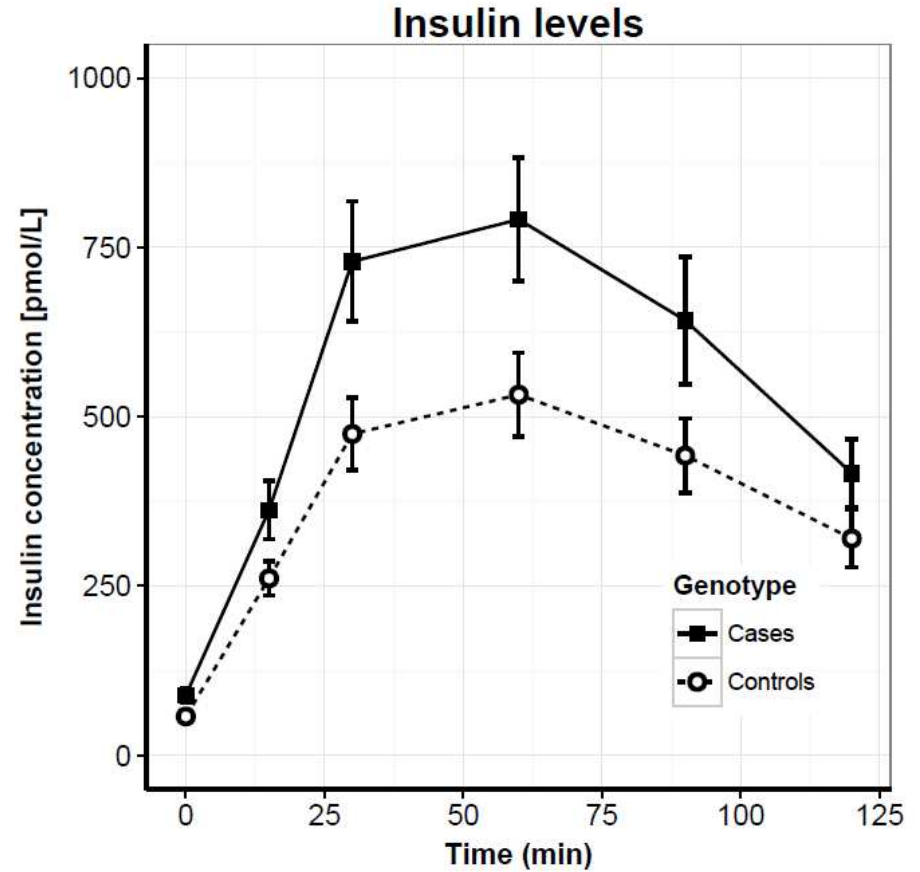
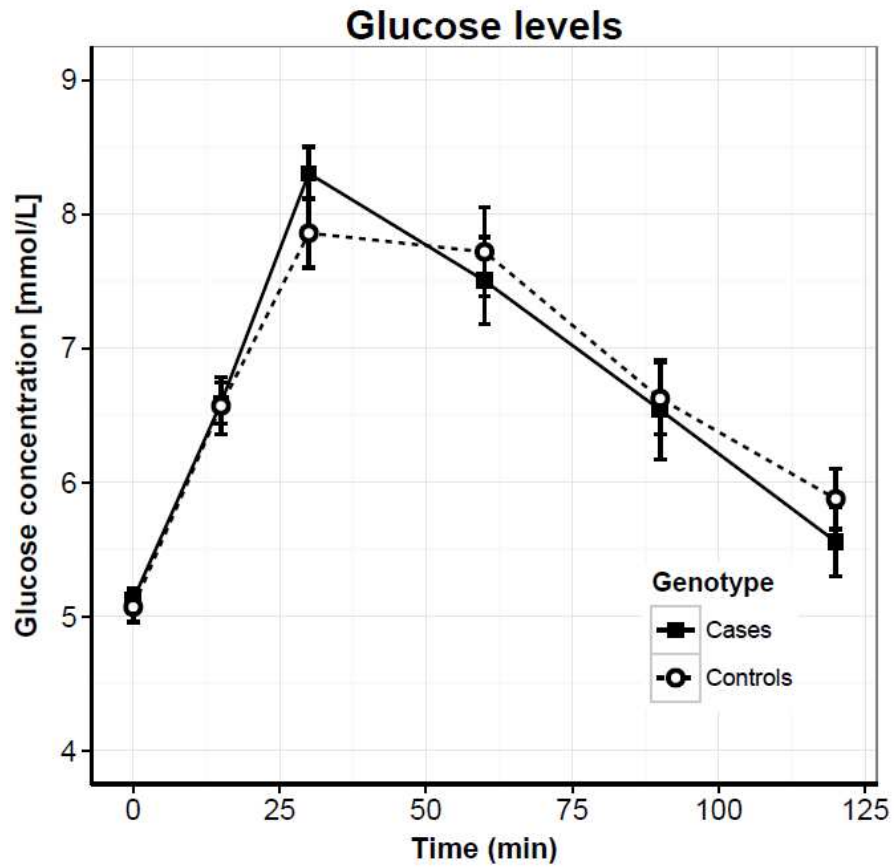
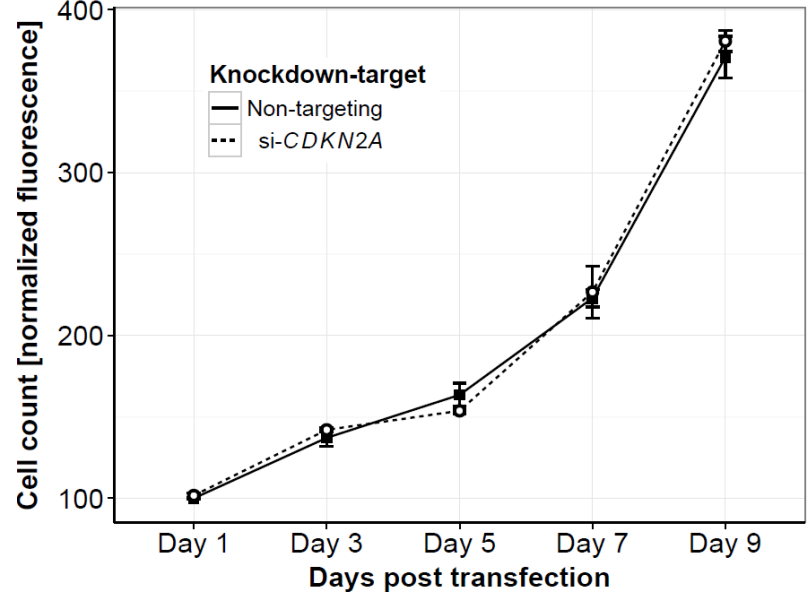
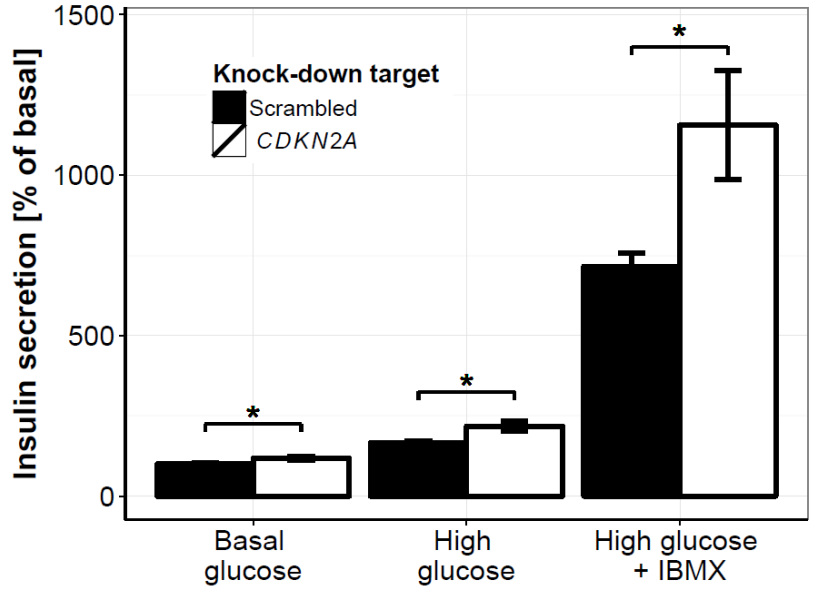
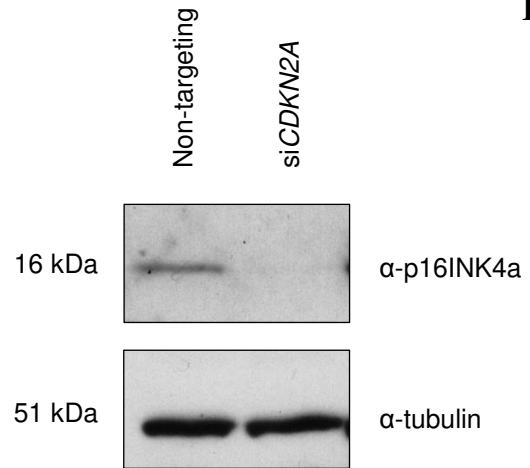
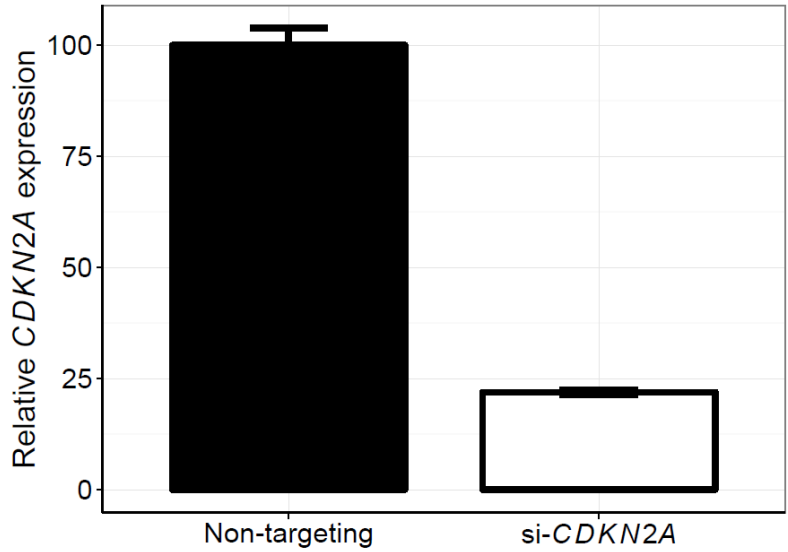


Figure 2



## Supplementary online information

Participant ID	Transcript affected	Mutation	Melanoma-free for > 2 years prior to study	Variant Effect Predictor (VEP - Ensembl)
OX_001	P16-INK4a only	c.88delG	Yes	Frameshift variant
OX_002	P16-INK4a only	c.88delG	Yes	Frameshift variant
OX_003	P16-INK4a only	c.88delG	Yes	Frameshift variant
OX_004	Both	c.458-105A>G	Yes	Intronic variant
OX_005	Both	c.458-105A>G	Yes	Intronic variant
OX_006	Both	c.458-105A>G	Yes	Intronic variant
OX_007	P16-INK4a only	c.52_57dup	Yes	Protein altering variant
OX_008	P16-INK4a only	c.52_57dup	Yes	Protein altering variant
OX_009	Both	c.159G>A	Yes	Missense variant
OX_010	Both	c.159G>A	Yes	Missense variant
OX_011	Both	c.458-105A>G	Yes	Intronic variant
OX_012	Both	<i>Not tested</i>	Yes	NA
LEI_001	Both	c.225_243del19	No	Frameshift variant
LEI_002	Both	c.225_243del19	Yes	Frameshift variant
LEI_003	Both	c.225_243del19	Yes	Frameshift variant
LEI_004	Both	c.225_243del19	Yes	Frameshift variant
LEI_005	Both	c.225_243del19	Yes	Frameshift variant
LEI_006	Both	c.225_243del19	Yes	Frameshift variant
LEI_007	Both	c.225_243del19	Yes	Frameshift variant
LEI_008	Both	c.225_243del19	Yes	Frameshift variant
LEI_009	Both	c.225_243del19	Yes	Frameshift variant

LEI_010	Both	c.225_243del19	Yes	Frameshift variant
LEI_011	Both	c.67G>C	No	Missense variant
LEI_012	Both	c.225_243del19	No	Frameshift variant
LEI_013	Both	c.225_243del19	Yes	Frameshift variant
LEI_014	Both	c.225_243del19	Yes	Frameshift variant
LEI_015	Both	c.225_243del19	Yes	Frameshift variant
LEI_016	Both	c.225_243del19	Yes	Frameshift variant
LEI_017	Both	c.225_243del19	Yes	Frameshift variant
LEI_018	Both	c.225_243del19	Yes	Frameshift variant
LEI_019	Both	c.225_243del19	Yes	Frameshift variant

**Supplementary table 1** List of mutations identified in carriers (annotated against CDKN2A-001 [ENST00000304494]) by targeted sequencing. The second column indicates whether the mutation maps to a region encoding just p16<sup>INK4a</sup> or both p16<sup>INK4a</sup> and p14<sup>ARF</sup>. Participant ID is an anonymous number assigned to each case, and the prefix indicates from which cohort the patient was recruited (OX = Oxford, UK; LEI = Leiden, Netherlands).

Measure/index	Parameter	Formula or mathematical model used	Reference
iHOMA-B	Beta-cell function	Computer model available via ( <a href="http://www.dtu.ox.ac.uk/homacalculator/">http://www.dtu.ox.ac.uk/homacalculator/</a> ).	(1)
iHOMA-S	Insulin sensitivity	Computer model available via ( <a href="http://www.dtu.ox.ac.uk/homacalculator/">http://www.dtu.ox.ac.uk/homacalculator/</a> ).	(1)
BIGTT-AIR <sub>0-30-120</sub>	Beta-cell function	$\exp[8.20 + (0.00178 * \text{insulin}_0) + (0.00168 * \text{insulin}_{30}) - (0.000383 * \text{insulin}_{120}) - (0.314 * \text{glucose}_0) - (0.109 * \text{glucose}_{30}) + (0.0781 * \text{glucose}_{120}) + (0.180 * \text{gender (where male=0 and female=1)}) - (0.032 * \text{BMI})]$	(2)
BIGTT-S <sub>I</sub> <sub>0-30-120</sub>	Insulin sensitivity	$\exp[4.90 - (0.00402 * \text{insulin}_0) - (0.000556 * \text{insulin}_{30}) - (0.00127 * \text{insulin}_{120}) - (0.152 * \text{glucose}_0) - (0.00871 * \text{glucose}_{30}) - (0.0373 * \text{glucose}_{120}) - (0.145 * \text{gender (where male=0 and female=1)}) - (0.0376 * \text{BMI})]$	(2)
Belfiore ISI	Insulin sensitivity	$2 / [(0.5 * \text{glucose}_0 + \text{glucose}_{60} + 0.5 * \text{glucose}_{120}) / 11.36] * (0.5 * \text{insulin}_0 + \text{insulin}_{60} + 0.5 * \text{insulin}_{120}) / 638 + 1]$	(3)
Matsuda ISI	Insulin Sensitivity	$10\,000 * \sqrt{(\text{glucose}_0 * \text{insulin}_0 * \text{glucose}_{\text{mean-OGTT}} * \text{insulin}_{\text{mean-OGTT}})}$	(4)
AUC	Multiple	Area under curve estimated using trapezoidal rule	(5)
Insulinogenic index	Beta-cell function	$(\text{insulin}_{30} - \text{insulin}_0) / (\text{glucose}_{30} - \text{glucose}_0)$	(6)
Disposition index	Beta-cell function	$\text{AUC}_{\text{insulin-OGTT}} / \text{AUC}_{\text{glucose-OGTT}} * \text{Matsuda ISI}$	(6)
Hepatic insulin clearance	Insulin clearance	$\text{AUC}_{\text{C-Peptide}} / \text{AUC}_{\text{Insulin}}$	(7)
Fasting insulin clearance	Insulin clearance	$\text{C-peptide}_0 / \text{insulin}_0$	(7)

**Supplementary table 2** Definitions of physiological measurements and indices derived from the OGTT. Subscripts denote time points during the OGTT. Units are pmol/L for insulin, nmol/L for C-peptide and mmol/L for glucose, except in the case of Matsuda ISI and the disposition index, where glucose was inputted in units of mg/dL and insulin as  $\mu\text{U/mL}$ .

	<b>Mutation carriers</b>	<b>Non-carriers</b>	<b>P-value</b>
n	28	31	NA
BMI [cm/kg <sup>2</sup> ]	27 [19, 38]	27 [19, 37]	0.66
Age [yrs]	51 [21, 71]	52 [25, 84]	0.96
Gender [% male]	43	33	0.58
Fasting glucose [mmol/L]	5.1 [4.3, 6.3]	5.1 [3.2, 6.4]	0.92
Fasting insulin [pmol/L]	91 [15, 337]	57 [22, 150]	0.01
iHOMA-B	133 [38, 452]	99 [45, 237]	0.03
iHOMA-S	86 [18, 329]	116 [35, 236]	0.04
BIGTT-AIR [*10 <sup>3</sup> ]	6.6 [0.9, 28]	3.2 [1.2, 12]	0.03
BIGTT-S	5.8 [0.4, 12.7]	7.5 [1.1, 17.8]	0.08
Belfiore ISI	0.80 [0.17, 1.35]	0.96 [0.35, 1.77]	0.03
Matsuda ISI	4.3 [0.8; 11.1]	6.1 [1.5; 20.9]	0.02
AUC <sub>glucose</sub>	831 [563, 1449]	832 [502, 1086]	0.98
AUC <sub>Insulin</sub> [*10 <sup>4</sup> ]	7.2 [2.4, 25]	4.9 [1.1, 15]	0.02
Insulinogenic index	205 [39, 561]	155 [53, 360]	0.10
Disposition index	2.3 [1.1, 3.8]	2.3 [1.0, 3.7]	0.92

**Supplementary table 3** Comparison of OGTT-derived measures for carriers and non-carriers after exclusion of three subjects that had presented with cancer within two years prior to the study (supplementary table 1). Data are given as mean and range [min; max], and p-values are from Welch's t-test, except for gender distribution where the Chi-squared test was performed. Details on definitions of physiological measures are listed in supplementary table 2. \* P-value < 0.05.

	<b>Mutation carriers</b>	<b>Non-carriers</b>	<b>P value</b>
n	8	8	NA
AUC <sub>insulin</sub> 0-10 min (pmol.L <sup>-1</sup> .min*10 <sup>-3</sup> )	4.8 [1.73, 13.2]	2.9 [1.84, 4.28]	0.51
AUC <sub>insulin</sub> 10-180 min (pmol.L <sup>-1</sup> .min*10 <sup>-3</sup> )	35.5 [13.7, 94.9]	16.9 [12.5, 22.2]	0.16
AUC <sub>C-peptide</sub> 0-10 min (pmol.L <sup>-1</sup> .min*10 <sup>-3</sup> )	15.1 [9.1, 31.9]	11.7 [5.5, 14.5]	0.96
AUC <sub>C-peptide</sub> 10-180 min (pmol.L <sup>-1</sup> .min*10 <sup>-3</sup> )	198 [103, 364]	152 [101, 186]	1.00
Net IVGTT insulin secretion 0-10 min (pmol.L <sup>-1</sup> )	0.56 [0.29, 0.84]	0.50 [0.10, 1.04]	0.65
Net IVGTT insulin secretion 10-180 min (pmol.L <sup>-1</sup> )	4.2 [1.20, 11.8]	2.8 [1.10, 4.98]	0.65
Insulin sensitivity, S <sub>I</sub> (min <sup>-1</sup> .pmol <sup>-1</sup> .L)	0.72 [0.19, 1.28]	0.68 [0.30, 0.95]	0.72
Disposition index [*10 <sup>-3</sup> ]	2.4 [1.14, 4.44]	1.9 [0.77, 3.40]	0.51
C-peptide disposition index	8.9 [3.45, 12.6]	7.8 [4.00, 13.7]	0.80
Fractional hepatic insulin throughput	0.53 [0.34, 1.12]	0.41 [0.26, 0.74]	0.23
Plasma insulin elimination rate (min <sup>-1</sup> )	0.098 [0.025, 0.207]	0.095 [0.042, 0.235]	0.72

**Supplementary table 4** IVGTT-derived measures of  $\beta$ -cell function, insulin sensitivity and hepatic clearance. Data are given as mean and range [min; max]. All p-values are based on Mann-Whitney U test.

## Supplementary figure legends

**Supplementary figure 1** Serum glucose (*left panel*) and insulin (*right panel*) levels during a 120-min OGTT in twenty-six cases with *CDKN2A* loss-of-function mutations affecting both p16<sup>INK4a</sup> and p14<sup>ARF</sup> (*black triangles, dotted line*), five cases with *CDKN2A* loss-of-function mutations affecting p16<sup>INK4a</sup> exclusively (*black squares, solid line*), and thirty-one BMI-, age-, and gender-matched controls (*white circles, dashed line*). Data shown as mean +/- SEM.

**Supplementary figure 2** Serum glucose (*left panel*) and insulin (*right panel*) levels during a 180-min IVGTT in eight carriers (*pink circles*) and eight BMI- ( $p = 0.72$ ), age- ( $p = 0.96$ ), and gender-matched ( $p = 0.50$ ) controls (*blue squares*). Data shown as mean +/- SEM.

**Supplementary figure 3** Immunofluorescence staining of p16INK4a (Abcam, ab81278; recognizing isoform 1 of the protein) in the human beta-cell line, EndoC-bH1. In siRNA-mediated knockdown experiments, expression of p16INK4a protein was visibly down-regulated (*bottom panel*) as compared with control cells (*top panel*). Cell nuclei were stained using NucRed Dead 647 (Life Technologies). Images were taken on a BioRad Radiance 2100 confocal microscope with a 60X 1.0 N.A. objective, and the same laser settings and intensities were used across samples. Scale bar, 20  $\mu\text{m}$ .

**Supplementary figure 4** Gene expression profiles of critical cell-cycle regulators after silencing of *CDKN2A* in the human  $\beta$ -cell line, EndoC-bH1. Knockdown experiments were performed as described for figure 2. Relative gene expression of *CDK4* (*top left*), *CDK6* (*top right*), *CDKN2A* (*bottom left*) and *CDKN2B* (*bottom right*) corrected for expression of two housekeepers using the delta-delta Ct method, and normalized to non-targeting control. As shown, we observed efficient knockdown of *CDKN2A* with no off-target effect on the *CDKN2B* gene. Bars represent means for  $n = 4-5$  and error bars are SEM.

**Supplementary figure 5** Insulin content normalized to cell-count following *CDKN2A* knockdown. After static insulin secretion assays, cells were counted and insulin contents extracted as described in figure 2. Using these data, the insulin content relative to the number of cells per well was calculated as the ratio between these two numbers, and normalized to scrambled control. Bars represent means for the aggregate of basal and high glucose measurements for  $n = 16$ , and error bars are SEM.

**Supplementary figure 6** PKA activity in the EndoC-bH1 cell line following *CDKN2A* knockdown. 96 h after treatment with non-targeting (“scrambled”; *blue bar*) or *CDKN2A* (*red bar*) siRNAs, cells were harvested and PKA activity measured on sample input normalized to cell numbers. Substrate conversion rates were calculated as the ratio of non-phosphorylated to total peptide using fluorescence intensities quantified with standard software on the ChemiDoc MP system. Data shown as mean +/- SEM for three independent replicates.

**Supplementary figure 7** Outline of two non-mutually exclusive mechanisms compatible with the phenotype of *CDKN2A* mutations-carriers. According to model 1 (*left*), a primary reduction in insulin sensitivity leads to a compensatory increase in insulin secretion to maintain glucose homeostasis. The effect of *CDKN2A*-loss would therefore be in non-beta cell tissues, such as liver. Model 2 (*right*), in contrast, represent the alternative scenario: chronically elevated insulin levels due to  $\beta$ -cell hypersecretion drives a progressive decrease in insulin receptors and insulin signalling through homologous desensitization (8). In this case, the primary effect of *CDKN2A* loss is on the pancreatic beta-cell, but the mechanism ultimately manifests as impaired insulin sensitivity and reduced insulin clearance. As discussed in the main text, it is likely that a combination of the two models contributes to both beta-cell hypersecretion and primary insulin resistance.

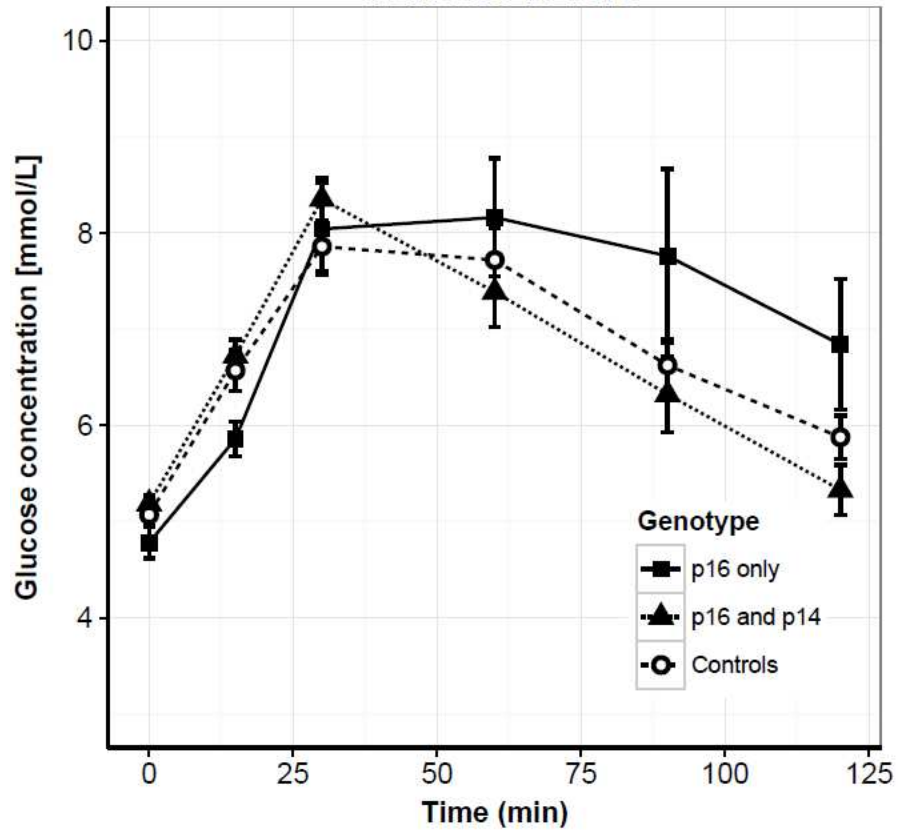
**Supplementary figure 8** Screenshot from the Human Islet Regulome Browser (9) showing annotations of chromatin state, transcription factor binding and variant association with type 2 diabetes at the *CDKN2A/B* locus. The genomic binding sites of islet transcription factors (PDX1, NKX2.2, FOXA2, NKX6.1, MAFB) are indicated by lines connected to the respective proteins. A Manhattan plot above shows log(p-values) of association with type 2 diabetes for variants in the MAGIC (*blue*) and DIAGRAM (*red*) datasets (10, 11). Lead variants tagging the two genome-wide association signals located downstream of *CDKN2B-AS1* are shown. Fine-mapping efforts have since publication of the islet regulome narrowed down the number of potential causative variants to credible sets of five and six variants (Gaulton et al, (2015) Nature Genetics, *in press*). Both of these sets contain variants that directly overlap a FOXA2 binding site.

## Supplementary references

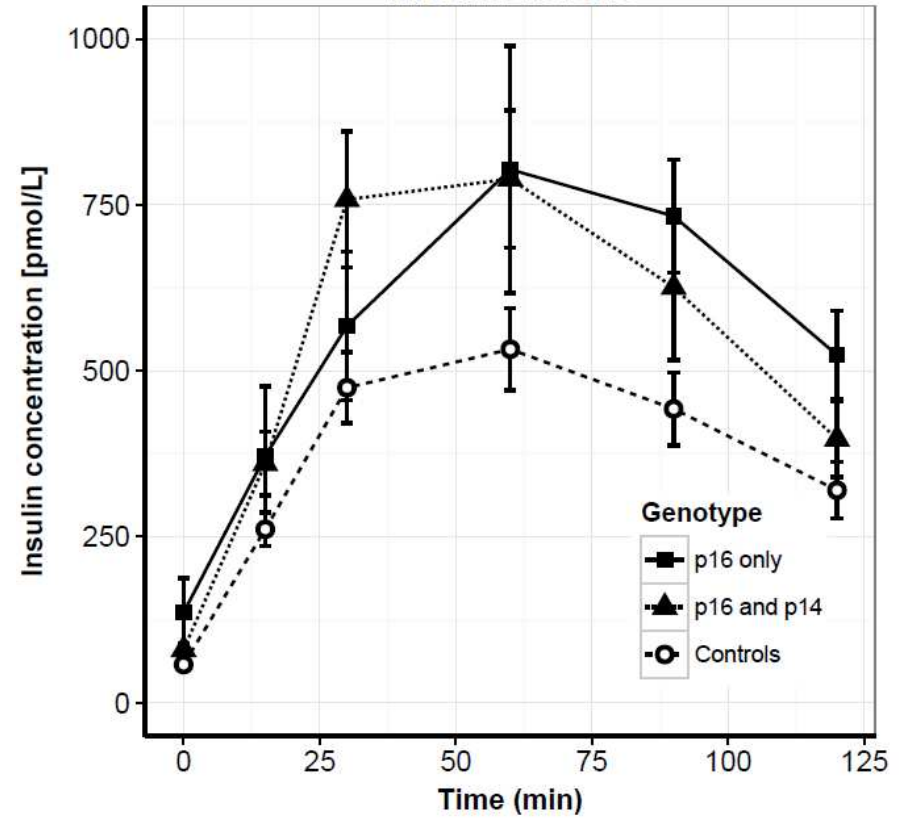
- 1 Matthews, D.R., *et al.* (1985) Homeostasis model assessment: insulin resistance and beta-cell function from fasting plasma glucose and insulin concentrations in man. *Diabetologia* 28, 412-419
- 2 Hansen, T., *et al.* (2007) The BIGTT test: a novel test for simultaneous measurement of pancreatic beta-cell function, insulin sensitivity, and glucose tolerance. *Diabetes Care* 30, 257-262
- 3 Belfiore, F., *et al.* (1998) Insulin sensitivity indices calculated from basal and OGTT-induced insulin, glucose, and FFA levels. *Mol Genet Metab* 63, 134-141
- 4 Matsuda, M. and DeFronzo, R.A. (1999) Insulin sensitivity indices obtained from oral glucose tolerance testing: comparison with the euglycemic insulin clamp. *Diabetes Care* 22, 1462-1470
- 5 Pacini, G. and Mari, A. (2003) Methods for clinical assessment of insulin sensitivity and beta-cell function. *Best Pract Res Clin Endocrinol Metab* 17, 305-322
- 6 Phillips, D.I., *et al.* (1994) Understanding oral glucose tolerance: comparison of glucose or insulin measurements during the oral glucose tolerance test with specific measurements of insulin resistance and insulin secretion. *Diabet Med* 11, 286-292
- 7 Herzberg-Schafer, S.A., *et al.* (2010) Evaluation of fasting state-/oral glucose tolerance test-derived measures of insulin release for the detection of genetically impaired beta-cell function. *PLoS One* 5, e14194
- 8 Shanik, M.H., *et al.* (2008) Insulin resistance and hyperinsulinemia: is hyperinsulinemia the cart or the horse? *Diabetes Care* 31 Suppl 2, S262-268
- 9 Pasquali, L., *et al.* (2014) Pancreatic islet enhancer clusters enriched in type 2 diabetes risk-associated variants. *Nat Genet* 46, 136-143
- 10 Morris, A.P., *et al.* (2012) Large-scale association analysis provides insights into the genetic architecture and pathophysiology of type 2 diabetes. *Nat Genet* 44, 981-990
- 11 Voight, B.F., *et al.* (2010) Twelve type 2 diabetes susceptibility loci identified through large-scale association analysis. *Nat Genet* 42, 579-589

Supplementary figure 1

## Glucose levels

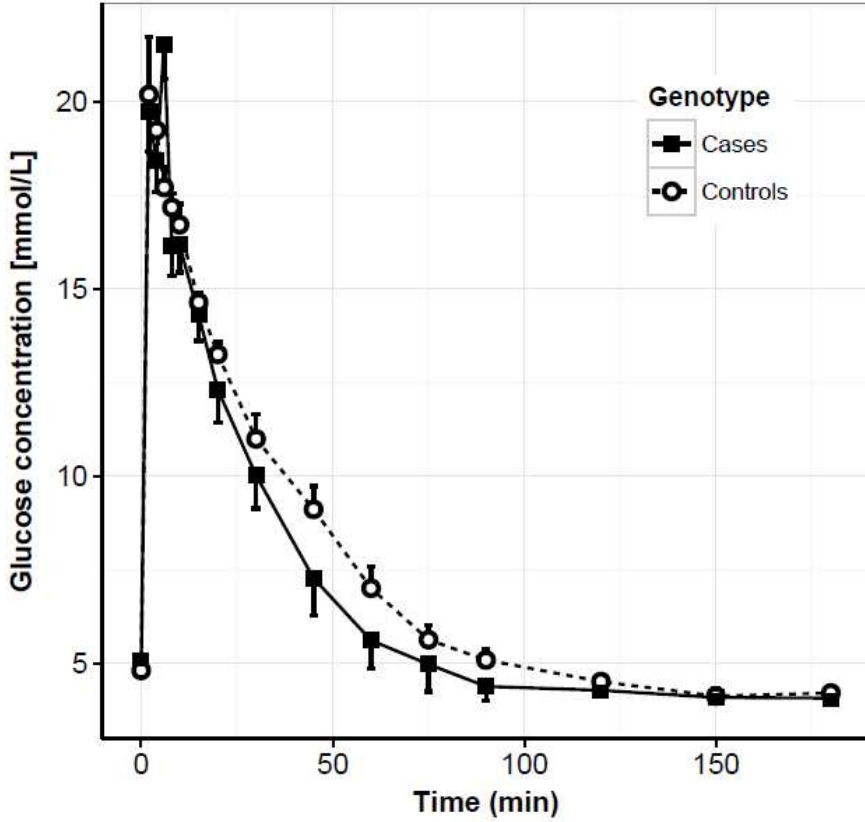


## Insulin levels

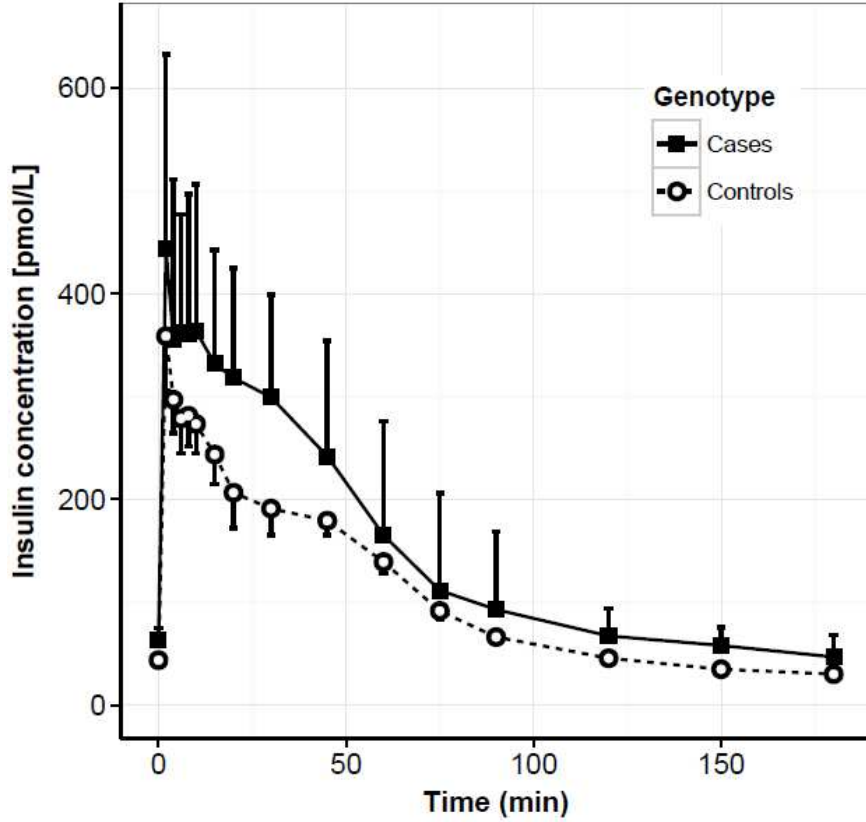


Supplementary figure 2

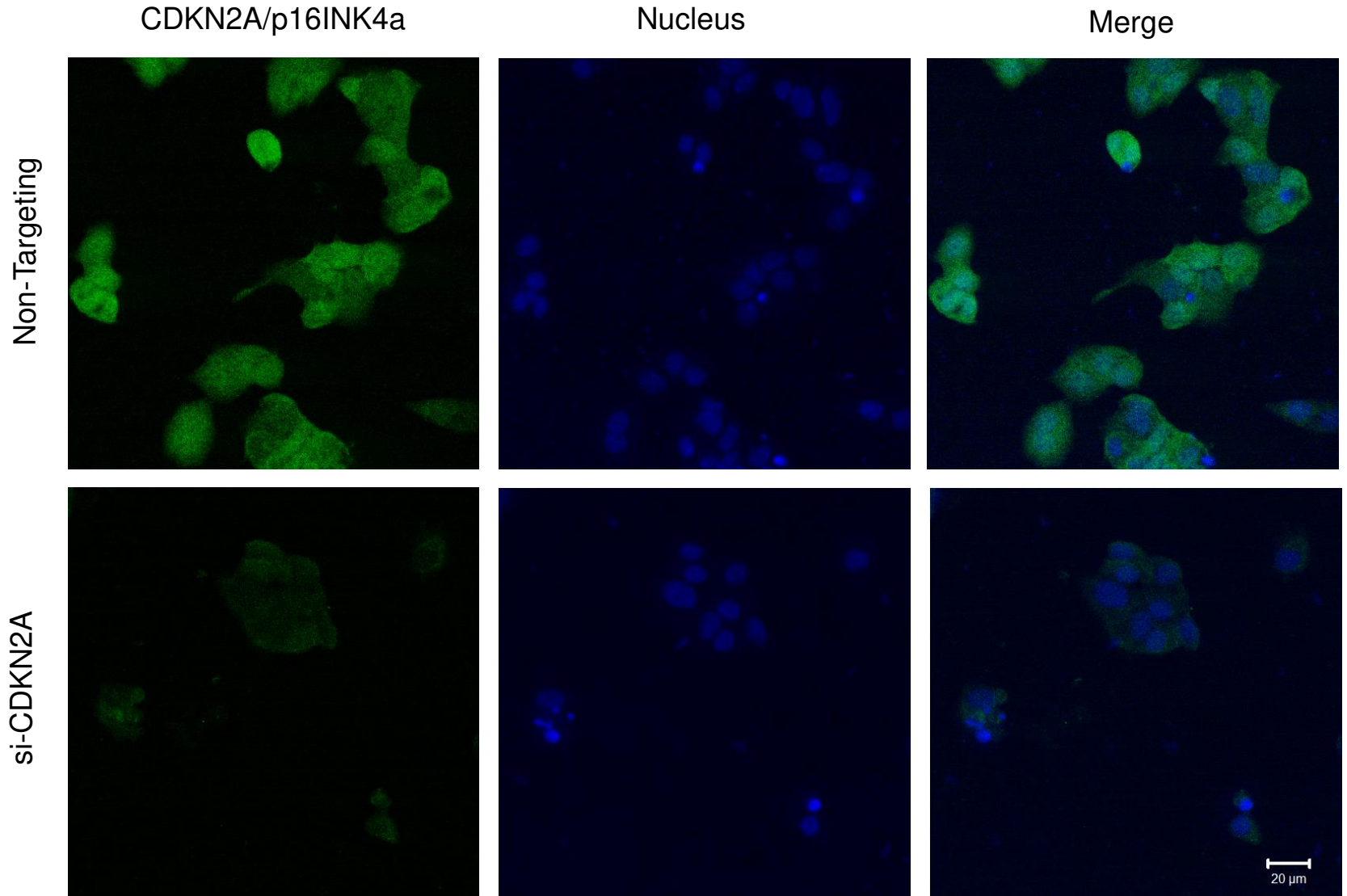
Glucose levels



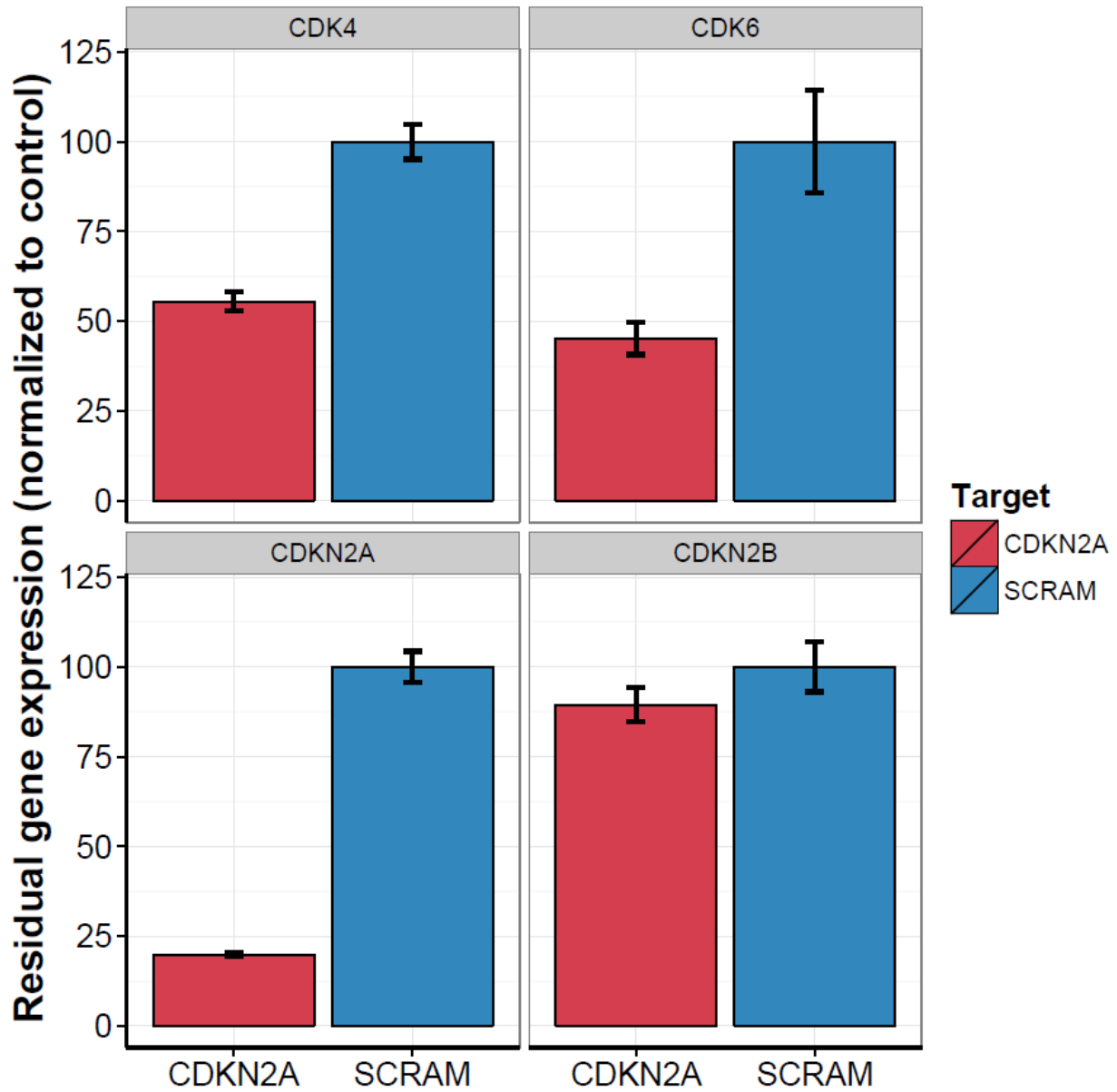
Insulin levels



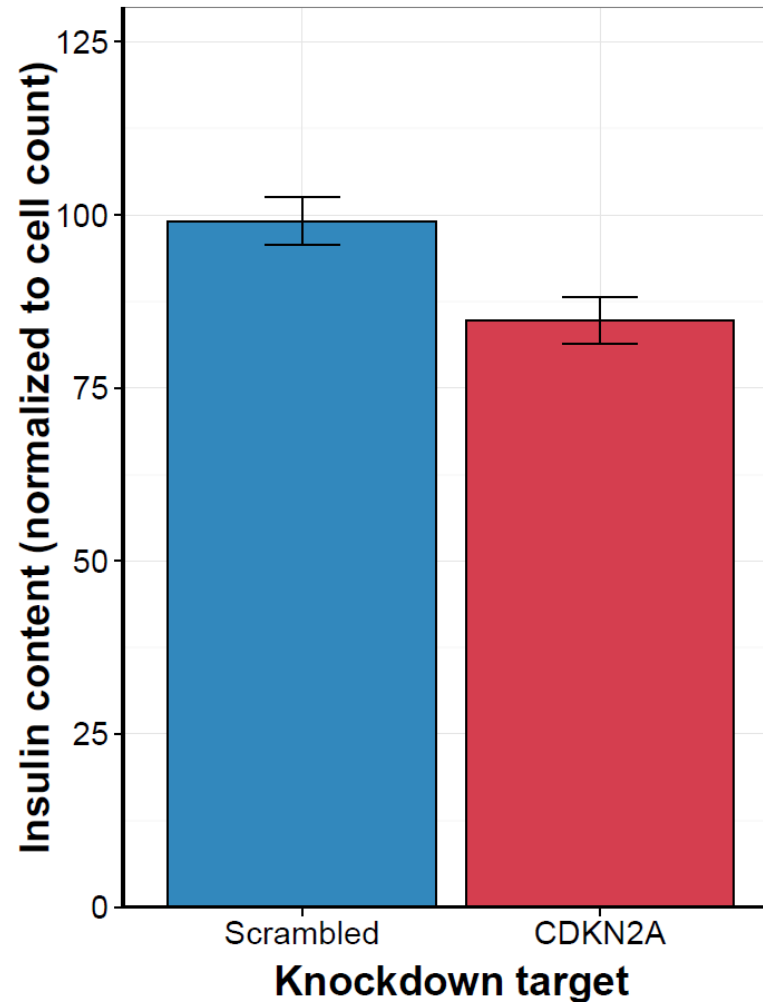
Supplementary figure 3



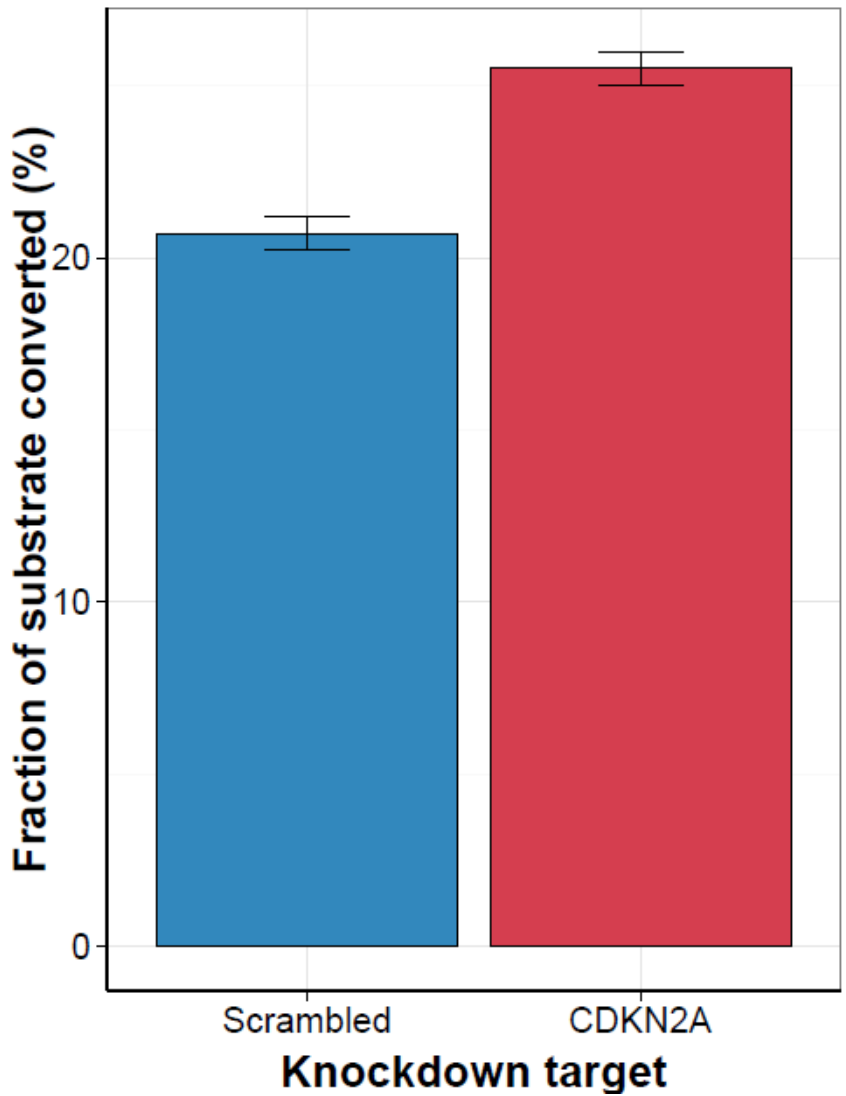
Supplementary figure 4



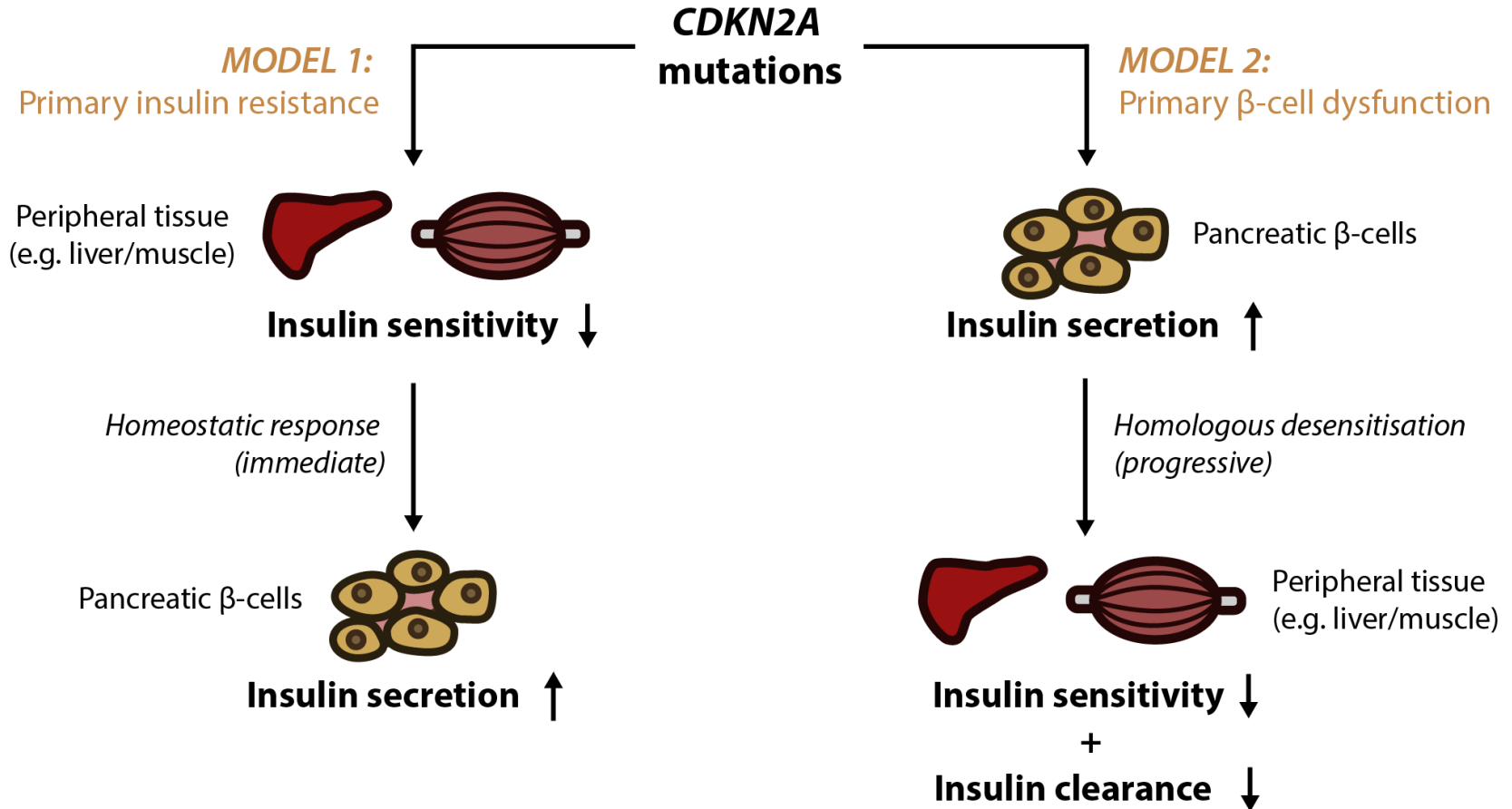
## Supplementary figure 5



Supplementary figure 6



## Supplementary figure 7



Supplementary figure 8

